

Original article

## Ship Collision Avoidance Path Planning Based on Particle Swarm Optimization and Neural Network in Bad Weather

Hu Yancai<sup>a</sup>, Gai Xudong<sup>b</sup>, Zhang Qiang<sup>c</sup>, and Liu Yang<sup>d</sup>

<sup>a</sup>Navigation and Shipping College, Shandong Jiaotong University, China, yancai@126.com

<sup>b</sup>Navigation and Shipping College, Shandong Jiaotong University, China, gaixudong1205@163.com

<sup>c</sup>Navigation and Shipping College, Shandong Jiaotong University, China, zq20060054@163.com, Corresponding Author

<sup>d</sup>Division of Maritime Transportation, Mokpo National Maritime University, Korea, 14915908@qq.com

### Abstract

Ship collision accidents not only endanger the safety of ships and personnel, but also may cause serious marine environmental pollution. To solve this problem, advanced technologies have been developed and applied in the field of intelligent ships in recent years. In this paper, a novel path planning algorithm is proposed based on particle swarm optimization (PSO) to construct a decision-making system for ship's autonomous collision avoidance using the process analysis which combines with the ship encounter situation and the decision-making method based on ship collision avoidance responsibility. This algorithm is designed to avoid both static and dynamic obstacles by judging the collision risk considering bad weather conditions by using BP neural network. When the two ships enter a certain distance, the optimal collision avoidance course and speed of the ship are obtained through the improved collision avoidance decision-making method. Finally, through MATLAB and Visual C++ platform simulations, the results show that the ship collision avoidance decision-making scheme can obtain reasonable optimal collision avoidance speed and course, which can ensure the safety of ship path planning and reduce energy consumption.

*Keywords: Collision avoidance, Decision-making algorithm, Particle swarm optimization, Ship path planning, BP neural network.*

## 1. Introduction

The intelligent shipping is to improve the traffic volume and speed, reduce costs and improve the overall efficiency of the industry. However, the occurrence of ship collision is accompanied by casualties, economic losses and ship damage. The research of intelligent collision avoidance path planning method plays an important role in intelligent navigation. To avoid ship collision, the intelligent path planning and collision avoidance decision-making has become an important research direction in the navigation field. PSO has received increasing attention in the optimization research community (Durillo, 2009), (Fernandez, 2011). In paper (Ding, 2014), a PSO variant on the basis of local stochastic search strategy (LSSPSO) was used to improve the performance of traditional PSO. Simulations of test functions demonstrate the improvement of LSSPSO in solving multiple benchmark problems. Further, to implement robot navigation in uncertain environment, Yong (2013) proposed a PSO multi-objective path planning algorithm. After that, the improved PSO algorithms were developed for path planning system (Das, 2016), (Mac, 2017), (Mistry, 2017).

For path planning and collision avoidance of unmanned surface vehicles (USV), ant colony algorithm was applied in the research of Agnieszka (2014) considering dynamic environment for intelligent decision-making of ships or intelligent obstacle detection and avoidance systems. For further research on multi-ship collision prevention, Zhang (2015) proposed a distributed, real-time decision support method. Collisions can be avoided if all ships comply with the COLREGs and some ships do not take action. In 2017, Liang Hu (2017) combined PSO algorithm with navigation rules by decomposing multi-ship collision avoidance into single-ship collision avoidance for online path planning. This algorithm provided a good solution to the multi-ship collision avoidance problem. Chen (2018), (2018) worked on collaborative collision avoidance of multi-vessels and the formation of ships by proposing the concept of Cooperative Multi-Vessel Systems (CMVSs) to solve the Vessel Train Formation (VTF) problem. In 2020 Chen (2020) further developed the CMVSs approach by including Cooperative Waterway Intersection Scheduling (CWIS).

Then hybrid algorithms of improved PSO have been expended in the researches (Wu, 2018), (Su, 2019), (Shao, 2020). Besides, fuzzy logic is widely applied for decision making method of collision avoidance in navigation by Perera (2014), Hu (2020), (2020). Based on COLREGS, Zhang (2021) proposed a method of collision avoidance actions before encounter situation and collision avoidance actions based on the different stages of the encounter situation. Considering path control for an USV, Guo (2020) studied a novel path following method of global path planning, taking advantage of the direction of currents. Chaotic and sharing-learning particle swarm optimization (CSPSO) algorithm was applied for the nonlinear multi-objective model.

Subsequently, Abhishek (2020) combined PSO and genetic algorithm to realize 3D path planning of UAV, which improved the convergence speed of the algorithm. To estimate the ship collision risk, Park (2022) aims to propose an enhanced machine learning method to estimate ship collision risk and to support decision-making for ship collision risk. The relevance vector machine (RVM) was applied to estimate the collision risk.

Based on the above literature analysis, many intelligent algorithms have been applied to the model of ship collision avoidance, and ship autonomous collision avoidance has become an indispensable part of intelligent ships (Akda, 2022). To make ship collision avoidance decisions more intelligent, closer to reality, and more accurate, this paper improves the efficiency of ship collision avoidance by improving PSO algorithm. Considering the applicability, regularity, safety and other characteristics of navigation, a ship collision avoidance system that conforms to COLREGs and judges whether to take collision avoidance actions independently is proposed to improve the safety of ships in the process of navigation at sea. The ship collision avoidance path simulation is conducted for open waters and narrow waters, respectively, to verify the reliability of the ship collision avoidance strategy.

The remainder of the paper is structured as follows. The second section is the theoretical basis. The dynamic collision avoidance model and method for ships based on polar coordinates is established in the third section. The fourth part firstly simulates the open water area

through MATLAB simulation platform, and verifies the reliability of the algorithm. Then the simulation experiment platform of ship collision avoidance developed on Visual C++ is adopted. The fifth section gives the conclusion of the paper.

## 2. Ship Collision Avoidance Theoretical Basis Preparation

### 2.1 Division of ship encountering situation and avoidance responsibility

According to COLREGs, the collision avoidance responsibilities between ships are determined according to the form of ship encounter which can be divided into three types: cross encounter (Target ships are located in Area A, Area B and Area E), overtaking (Target ships are located in Area C and Area D), and encounter (Target ships are located in Area F), as shown in Fig. 1.

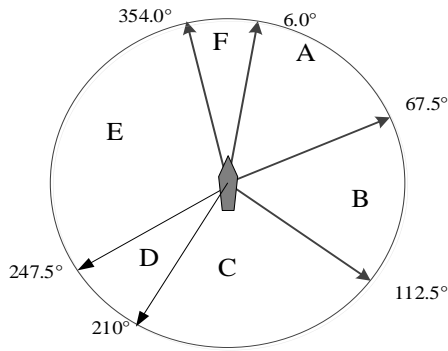


Figure 1. Classification of ship encounter situation

### 2.2 Ship motion parameters

In the research of ship collision avoidance methods, when a ship is sailing in open waters, whether there is a risk of collision between two ships is generally judged by using the dynamic and static information between the ship and other ships, including relative orientation, relative course, speed and distance between two ships, to calculate relevant motion parameters. According to the rules, it is compared with the safety threshold obtained from collision avoidance research.

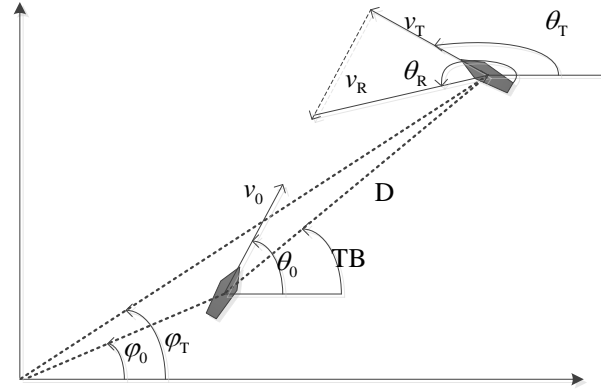


Figure 2. Schematic diagram of relative motion for ships

The position of the ship is defined as  $(p_0, \varphi_0)$ . The ship speed is  $v_0$ . Course is  $\theta_0$ . The initial position of the target ship is  $(p_T, \varphi_T)$ . Target ship speed is  $v_T$ . Target ship course is  $\theta_T$ . The relative motion of two ships is shown in Fig. 2.

Let

$$\Delta x = p_T \cos \varphi_T - p_0 \cos \varphi_0, \Delta y = p_T \sin \varphi_T - p_0 \sin \varphi_0 \quad (1)$$

The distance between the ship and the target ship is

$$D = \sqrt{(\Delta x^2 + \Delta y^2)} \quad (2)$$

The speed components of the ship and the target ship on the x-axis and y-axis are

$$v_{x0} = v_0 \cos \theta_0, v_{y0} = v_0 \sin \theta_0 \quad (3)$$

$$v_{xT} = v_T \cos \theta_T, v_{yT} = v_T \sin \theta_T \quad (4)$$

The components of the target ship's speed relative to its own ship on the x and y axes are

$$v_{xR} = v_{xT} - v_{x0}, v_{yR} = v_{yT} - v_{y0} \quad (5)$$

$$v_R = \sqrt{v_{xR}^2 + v_{yR}^2} \quad (6)$$

The course of the moving target ship relative to the own ship is

$$\theta_R = \begin{cases} 90^\circ & v_{xR} = 0, v_{yR} \geq 0 \\ 270^\circ & v_{xR} = 0, v_{yR} < 0 \\ \arctan v_{yR} / v_{xR} & v_{xR} > 0, v_{yR} \geq 0 \\ 180^\circ + \arctan v_{yR} / v_{xR} & v_{xR} < 0 \\ 360^\circ + \arctan v_{yR} / v_{xR} & v_{xR} > 0, v_{yR} < 0 \end{cases} \quad (7)$$

The true bearing (TB) of the target ship relative to the own ship is

$$TB = \begin{cases} 90^\circ & \Delta x = 0, \Delta y \geq 0 \\ 270^\circ & \Delta x = 0, \Delta y < 0 \\ \arctan \Delta y / \Delta x & \Delta x > 0, \Delta y \geq 0 \\ 180^\circ + \arctan \Delta y / \Delta x & \Delta x < 0 \\ 360^\circ + \arctan \Delta y / \Delta x & \Delta x > 0, \Delta y < 0 \end{cases} \quad (8)$$

Distance to the closest point of approach (DCPA) of target ship is positive when passing the bow of the ship and negative when passing the stern. DCPA and Time to the closest point of approach (TCPA) can be divided into the following two cases. For ships coming from starboard side that

$$DCPA = D \sin(\theta_R - TB - 180^\circ) \quad (9)$$

$$TCPA = D \cos(\theta_R - TB - 180^\circ) / v_R \quad (10)$$

For ships coming from port side that  $0^\circ < \theta_R \leq 90^\circ$  or  $270^\circ < \theta_R \leq 360^\circ$

$$DCPA = D \sin(TB - \theta_R - 180^\circ) \quad (11)$$

$$TCPA = D \cos(TB - \theta_R - 180^\circ) / v_R \quad (12)$$

When the absolute value of DCPA is less than 2 n miles and TCPA is greater than 0 and less than 0.4 h, it can be determined that there is a risk of collision between two ships. When TCPA is less than 0, it means that the distance between the two ships is getting larger, then there is no risk of collision between the two ships.

### 2.3 The improved PSO algorithm

In this paper, the particle convergence speed of the algorithm is improved by using the inertia weight  $\omega$  which is a scale factor related to the speed at the previous time, and the speed update equation is elaborated in equation (13).

$$v_{i,d}(t+1) = \omega v_{i,d}(t) + c_1 r_1 (P_{i,d}(t) - x_{i,d}(t)) + c_2 r_2 (P_{g,d}(t) - x_{i,d}(t)) \quad (13)$$

$$x_{i,d}(t+1) = x_{i,d}(t) + v_{i,d}(t+1) \quad (14)$$

The calculation of inertia weight  $\omega$  is

$$\omega = \omega_{\max} - ((\omega_{\max} - \omega_{\min}) \text{run} / \text{run}_{\max} + p) \quad (15)$$

where the maximum inertia weight  $\omega_{\max}$  is generally 0.9. The minimum inertia weight  $\omega_{\min}$  is generally 0.4.

$\text{run}$  is the current number of iterations.  $p$  is a regulating factor.  $\text{run}_{\max}$  is the total number of iterations.

The value of learning factors  $c_1$  and  $c_2$  are generally set as an equal constant. When the value is between 0 and 4, a better solution can be found. After consulting the data and verifying for many times, both the value of  $c_1$  and  $c_2$  are taken as 2.0.

For improving the ability to jump out of the local optimal solution, it is necessary to give particles a larger inertia weight in the early stage to enhance the particle's ability to find the local optimal solution, and in the later stage of the search, it is necessary to enhance the particle's local optimization ability and give particles a smaller inertia weight. Therefore, the relationship between global optimization and local optimization has been considered based on balance considerations. When the value range of  $p$  is [0.6,0.9] and the particle iterates once, that is  $\text{run} = \text{run} + 1$ , the adjustment factor increases linearly in the way  $p = p + 0.3 / \text{run}_{\max}$ .

### 3. Ship Collision Avoidance Method Based on Improved PSO Algorithm

In the research of relevant papers, ship collision avoidance decisions are often made by steering. The collision avoidance decision-making system in this paper is based on the improved PSO algorithm, which takes the relative azimuth, distance, relative speed, DCPA, TCPA and other parameters formed by target ships and their own ships as the input values to obtain more effective and reasonable steering angles.

#### 3.1 Collision avoidance model of dynamic obstacles

The geometric modeling of ship (S) and circular dynamic obstacle at the current time is shown in Fig. 3. As it is inevitable to take into account some uncertain factors, such as the uncertainty of the ship's own navigation movement, the uncertainty of the movement of other ships, the uncertainty of the movement of obstacles other than the ship, and the error of the detection and positioning system for target ships or other obstacles. For the above reasons, the ship is treated as a centroid to simplify the calculation.

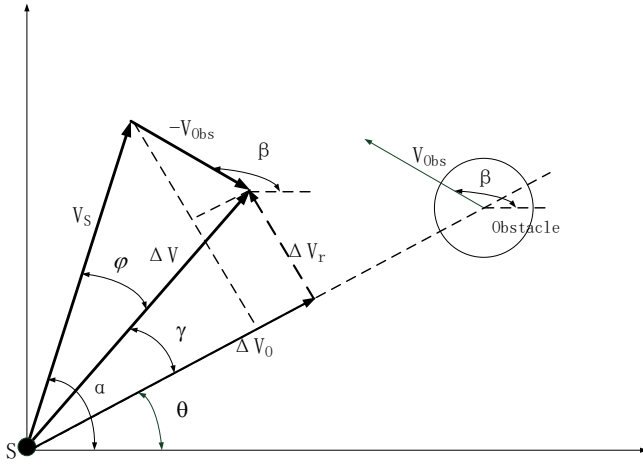


Figure 3. Parameters between own ship and target ship

In Fig. 3,  $V_S$  is the motion speed of the S.  $V_{Obs}$  is the movement speed of the obstacle.  $e_x$  is the polar axis,  $L_{RO}$  is the line between the S and the center of the obstacle circle,  $L_q$  is the tangent line of the obstacle circle, and  $\Delta V$  is the speed of the S relative to the obstacle.  $\alpha = \angle(V_S, e_x)$  is the angle from the polar axis to  $V_S$ , and  $\beta = \angle(V_{Obs}, e_x)$  is the angle from the polar axis to  $V_{Obs}$ .  $\theta = \angle(L_{RO}, e_x)$  is the angle from the polar axis to the line  $L_{RO}$  connecting the S and the center of the obstacle circle,  $\varphi = \angle(V_S, \Delta V)$  is the angle  $\Delta V$  to  $V_S$ ,  $\gamma = \angle(\Delta V, L_{RO})$  is the angle  $\Delta V$  to  $L_{RO}$ , and  $\mu = \angle(L_{RO}, L_q)$  is the angle from the tangent line  $L_q$  of the obstacle circle to  $L_{RO}$ . To enable the ship to avoid the obstacle zone at the next moment,  $\gamma$  should be angle outside of  $(\theta - \mu, \theta + \mu)$ .

The speed and course for the ship collision avoidance can be obtained by solving  $\gamma$ . The velocity triangle formed by  $V_S$ ,  $\Delta V$  and  $V_{Obs}$  is used to solve  $\gamma$  and  $\Delta V_r$ .

$$\begin{cases} \Delta V_r = V_S \sin(\alpha - \theta) - V_{Obs} \sin(\beta - \theta) \\ \Delta V_o = V_S \cos(\alpha - \theta) - V_{Obs} \cos(\beta - \theta) \end{cases} \quad (16)$$

In Formula (16),  $\Delta V$  can be decomposed into the vertical velocity component  $\Delta V_o$  and the velocity component  $\Delta V_r$  pointing to the center of the obstacle. The value of  $\gamma$  is shown as

$$\gamma = \arctan\left(\frac{V_S \sin(\alpha - \theta) - V_{Obs} \sin(\beta - \theta)}{V_S \cos(\alpha - \theta) - V_{Obs} \cos(\beta - \theta)}\right) \quad (17)$$

Let

$$f = f(V_S, \alpha, V_{Obs}, \beta) = \frac{V_S \sin(\alpha - \theta) - V_{Obs} \sin(\beta - \theta)}{V_S \cos(\alpha - \theta) - V_{Obs} \cos(\beta - \theta)} \quad (18)$$

$$d\gamma = d(\arctan f(V_S, \alpha, V_{Obs}, \beta)) = \frac{1}{1 + f^2} df \quad (19)$$

The function  $f$  is a coincidence function, and its integral is multiplied by its derivative in Formula (19).

$$\frac{1}{1 + f^2} = \frac{1}{1 + \left[ \frac{V_S \sin(\alpha - \theta) - V_{Obs} \sin(\beta - \theta)}{V_S \cos(\alpha - \theta) - V_{Obs} \cos(\beta - \theta)} \right]^2} \quad (20)$$

$$\begin{aligned} &= \frac{[V_S \cos(\alpha - \theta) - V_{Obs} \cos(\beta - \theta)]^2}{V_S^2 + V_{Obs}^2 - 2V_S V_{Obs} \cos(\alpha - \beta)} \\ df &= df(V_S, \alpha, V_{Obs}, \beta) = \frac{\partial f}{\partial V_S} dV_S \\ &+ \frac{\partial f}{\partial \alpha} d\alpha + \frac{\partial f}{\partial V_{Obs}} dV_{Obs} + \frac{\partial f}{\partial \beta} d\beta \end{aligned} \quad (21)$$

Formula (21) is to differentiate each variable in Formula (19). Assuming that there is no sudden change in the movement of circular obstacles, the change of their speed  $V_{Obs}$  and direction  $\beta$  of movement is negligible in a very short time, thus  $dV_{Obs} = 0$ ,  $d\beta = 0$ .

$$\frac{\partial f}{\partial V_S} dV_S = \frac{V_S \sin(\beta - \alpha)}{[V_S \cos(\alpha - \theta) - V_{Obs} \cos(\beta - \theta)]^2} dV_S \quad (22)$$

$$\frac{\partial f}{\partial \alpha} d\alpha = \frac{V_S^2 - V_{Obs} V_S \cos(\alpha - \beta)}{[V_S \cos(\alpha - \theta) - V_{Obs} \cos(\beta - \theta)]^2} d\alpha \quad (23)$$

$$\begin{aligned} df &= \frac{V_S \sin(\beta - \alpha)}{[V_S \cos(\alpha - \theta) - V_{Obs} \cos(\beta - \theta)]^2} dV_S \\ &+ \frac{V_S^2 - V_{Obs} V_S \cos(\alpha - \beta)}{[V_S \cos(\alpha - \theta) - V_{Obs} \cos(\beta - \theta)]^2} d\alpha \end{aligned} \quad (24)$$

Substitute Formula (24) and Formula (20) into Formula (19), it has

$$\begin{aligned} d\gamma &= \frac{V_S \sin(\beta - \alpha)}{V_S^2 + V_{Obs}^2 - 2V_S V_{Obs} \cos(\alpha - \beta)} dV_S + \\ &\frac{V_S^2 - V_{Obs} V_S \cos(\alpha - \beta)}{V_S^2 + V_{Obs}^2 - 2V_S V_{Obs} \cos(\alpha - \beta)} d\alpha \end{aligned} \quad (25)$$

$$\begin{aligned} \Delta\gamma &= \frac{V_S \sin(\beta - \alpha)}{V_S^2 + V_{Obs}^2 - 2V_S V_{Obs} \cos(\alpha - \beta)} \Delta V_S + \\ &\frac{V_S^2 - V_{Obs} V_S \cos(\alpha - \beta)}{V_S^2 + V_{Obs}^2 - 2V_S V_{Obs} \cos(\alpha - \beta)} \Delta\alpha \end{aligned} \quad (26)$$

There is a relationship (27), where  $\varphi$  is the angle between  $V_S$  and  $\Delta V$ .

$$\begin{cases} V_{Obs} \sin(\beta - \alpha) = \Delta V \sin \varphi \\ V_S - V_{Obs} \cos(\beta - \alpha) = \Delta V \cos \varphi \\ V_S^2 + V_{Obs}^2 - 2V_S V_{Obs} \cos(\alpha - \beta) = \Delta V^2 \end{cases} \quad (27)$$

Substituting Formula (27) into (26), we can get

$$\Delta\gamma = \frac{-\sin\varphi}{\Delta V} \Delta V_s + \frac{V_s \cos\varphi}{\Delta V} \Delta\alpha \quad (28)$$

It can be seen from Formula (28) that the speed  $\Delta V_s$  and course  $\Delta\alpha$  of the ship (S) can be adjusted to change value of  $\Delta\gamma$ , that is,  $\Delta V_s$  and  $\Delta\alpha$  correspond to two effective collision avoidance maneuvering s of the ship (S) respectively. To make the ship (S) escape from the collision danger area  $(\theta - \mu, \theta + \mu)$ ,  $\Delta\gamma$  has to meet the condition bellow.

$$\begin{cases} \Delta\gamma \geq \mu - \gamma & \gamma > 0 \\ \Delta\gamma \leq -(\mu + \gamma) & \gamma < 0 \end{cases} \quad (29)$$

### 3.2 Fitness function of dynamic collision avoidance

In the course of navigation, ships rarely change their speed, but more often change their course. In the case of collision avoidance, it is necessary to change the speed and navigation strategy at the same time. In the improved PSO algorithm, the change of ship speed and course in collision avoidance is taken as two dimensions values, so the ship collision avoidance path planning problem can be expressed as a goal optimization problem under multiple conditions.

$$\begin{cases} f(\Delta V_s, \Delta\alpha) = m_1 |\Delta V_s| + m_2 |\Delta\alpha| \\ \frac{-\sin\varphi}{\Delta V} \Delta V_s + \frac{V_s \cos\varphi}{\Delta V} \Delta\alpha \geq \mu - \gamma \quad (\gamma \geq 0) \\ \frac{-\sin\varphi}{\Delta V} \Delta V_s + \frac{V_s \cos\varphi}{\Delta V} \Delta\alpha < \mu - \gamma \quad (\gamma < 0) \end{cases} \quad (30)$$

where  $\varphi, \mu, \gamma$  and  $\Delta V$  are known.  $f(\Delta V_s, \Delta\alpha)$  is the objective function of the optimal solution, that is, the fitness function in the PSO algorithm. Each updated particle needs to judge whether it is within the navigable region, otherwise the optimal solution will not be updated. The optimal solution thus obtained can meet the requirements of the COLREGs and not intersect with static obstacles. If there are multiple dynamic obstacles in the path of the ship, it is only necessary to add the second and third constraints in Formula (30) to each obstacle.

The input data for collision avoidance is obtained through devices on the ship or other ways, including the heading, speed, coordinates, ship size and shape and other values of the ship and target ships. The judgment of whether there is collision risk shall be divided

according to the environment of the ship. In the open water, it is determined by calculating the TCPA and DCPA values between the ship and target ships. When  $0\text{min} < \text{TCPA} < 12\text{min}$  and  $|\text{DCPA}| < 2\text{n mile}$ , there is a risk of collision between the two ships. In the narrow water, it is determined by whether the ship will enter the expansion model of target ships or obstacles. If the original path of the ship will enter the model area, there is a risk of collision. The judgment of navigable region includes COLREGs and ship collision avoidance situation division. The positive value of course change is left steering, the negative value of course change is right steering, the positive value of speed change is acceleration, and the negative value of speed change is decrease.

### 3.3 Modeling of obstacles and ships for collision avoidance in bad weather

In open waters, this paper expands the obstacle ship into a circle with a radius of 2 n miles based on the DCPA safety threshold of 2 n miles. Although some navigable areas are lost, the navigable areas are large in open waters and the loss of navigable areas is to ensure the encounter safety, thus it is a reasonable. In narrow waters, more considerations are given to navigable areas. Therefore, considering the shape of obstacles or obstacle ships, the following two modeling methods are adopted (Xiang Zuquan, 2015).

(1) For an object with length to width ratio greater than 2:1, the oriented bounding box (OBB) is used to simulate the object, and it is more closely to the actual shape. Although the amount of calculation is high, relatively more effective paths can be obtained through calculation, which help produce a better collision avoidance path and adapt to the environment of narrow waters.

(2) For an object with length to width ratio less than 2:1, the circle is used to enclose it without losing too much navigable path and simplify the calculation. The specific value of the outer circle takes the maximum value of all the fixed points of the object.

The expanding method has been implemented in paper (Du Kaijun, 2015), in which the value of security threshold  $\rho$  is set as five times of ship length. However, the weather conditions are not taken into account. Under the conditions of bad weather, the vulnerability of collision increases. To improve safety of collision

avoidance, the main factors wind speed (WS) and wave height (WH) are taken into consideration as input variables. BP neural network is applied to predict the increment of expanding value of coefficient  $\xi$ . Thus, expanding value incorporates security threshold of five times of ship length and expanding increment due to bad weather conditions. The input vector has 2 elements and the output vector has 1 element, so there are 2 neurons in the input layer of the network and 1 neuron in the output layer. The expanding value  $\varepsilon$  is designed as

$$\varepsilon = \vartheta + \xi * \vartheta \tag{31}$$

**4.Simulations**

In order to verify the ship collision avoidance decision based on improved PSO, MATLAB software is used to compile simulation program to verify the effectiveness of this method. The collision avoidance speed and angle are calculated by collecting the polar diameter, polar angle, speed and sailing direction of target ships within the ship's detection range.

*4.1 Numerical simulation verification*

To prove the applicability and effectiveness of the

improved PSO algorithm, this paper verifies the algorithm through Schaffer function. The specific function is shown in Formula (32).

$$f(x, y)_{\max} = 0.5 + \frac{(\sin \sqrt{x^2 + y^2})^2 - 0.5}{[1 + 0.001(x^2 + y^2)]^2} \tag{32}$$

In this calculation, the population quantity of the PSO algorithm is 100, the learning factors  $c_1, c_2$  are 2.0, and the number of iterations of the algorithm is 50. Schaffer function is a classical verification function, and there are many local optimal solutions. The particles in this paper can fall into the global optimal solution area. It can be seen that the improved algorithm in this paper can avoid falling into the local optimal solution. The algorithm can get the optimal solution in about six iterations, which shows that the algorithm has excellent optimization ability.

In the simulation, there are 30 groups of data in Table 1, six of which are test samples, the remaining 24 groups of data are used as training sample sets. Trainlm learning algorithm is selected. Input number is hidden number is 5 and the output number is 1.

**Table 1 Training data of BP neural network**

VARIABLES	TRAINING DATA															
WS M/S	9	9	9	9	9	10	10	10	10	10	11	11	11	11	11	
WH M	1	1.5	2	2.5	3	1	1.5	2	2.5	3	1	1.5	2	2.5	3	
$\xi$	0.37	0.44	0.56	0.65	0.72	0.39	0.46	0.56	0.65	0.75	0.46	0.53	0.60	0.68	0.78	
WS M/S	12	12	12	12	12	13	13	13	13	13	9	10	11	12	13	
WH M	1	1.5	2	2.5	3	1	1.5	2	2.5	3	1	1.5	2	2.5	3	
$\xi$	0.51	0.58	0.65	0.71	0.81	0.56	0.63	0.71	0.75	0.88	0.37	0.46	0.60	0.71	0.88	

The number of training times is set to 1000. The learning rate is set to 0.01 and the minimum error of training target is set as 0.00001. Predicted value and expected value are shown in Fig.4 using BP neural network. The neural network training regression is shown in Fig. 5.

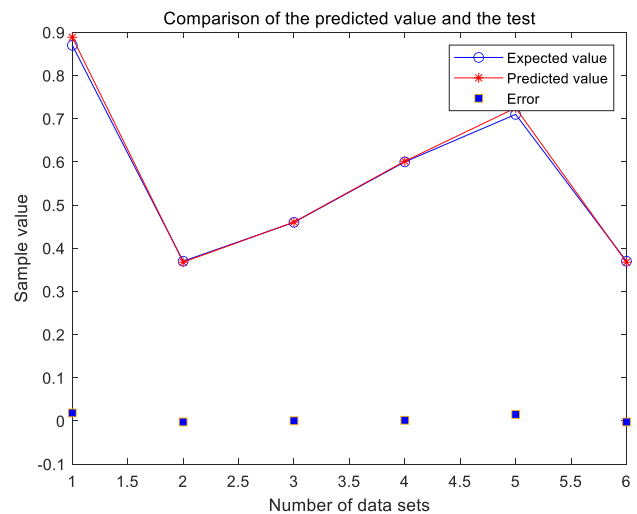


**Figure 4 Predicted and expected values**

The WS and WH condition of bad weather are set as (11.5m/s, 1.75m), the predicting results of the BP

neural network is 0.58.

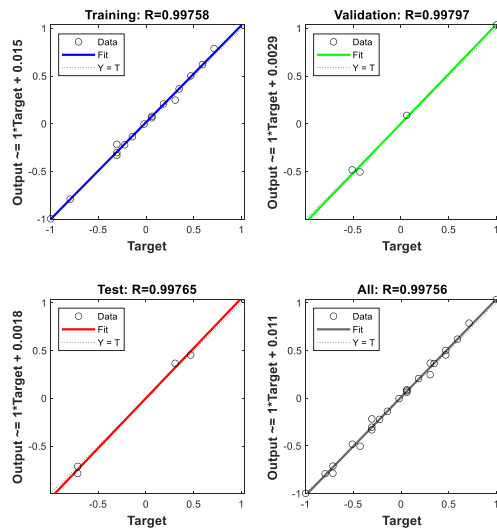


Figure 5 Neural network training regression

4.2 Simulation of ship collision avoidance in open waters

In this paper, the encounter situation between three ships is simulated. The initial position, sailing speed and direction angle of each ship in the forward coordinate are shown in Table 2, and the encounter situation between ships is shown in Fig. 6.

Table 2 Ship parameters

SHIP	POLAR DIAMETER/R/N MILE	POLAR ANGLE/(°)	SPEED/KN	BEARING ANGLE/(°)
S	0	0	40	0
TS1	4	30	30	270
TS2	6	0	20	180
TS3	6	0	16	217.8

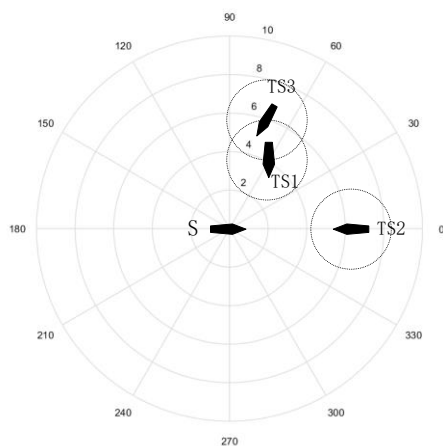


Figure 6 Initial encounter situation

From the analysis of Table 1 and Fig. 5, it can be seen that if the three target ships comply with

COLREGs, the ship needs to give way to TS2, but when taking collision avoidance measures, the ship needs to consider reducing the risk of collision with TS1 and TS3. The problem can be converted into that the ship S finds the optimal heading to avoid collision with TS2. The PSO algorithm is to plan the collision avoidance path between the ship S and the target ship TS1, TS2, TS3. DCPA and TCPA data between the ship and the three target ship are shown in Table 3.

Table 3 DCPA and TCPA of ship encounter

TCPA, DCPA	S and TS1	S and TS2	S and TS3
TCPA/min	4.2	6	3.2
DCPA/n mile	0.6	0	5.2

The number of particle swarm of the algorithm is set as 100, and the number of iterations is set as 100. In the fitness function, m1 is set to 1 and m2 is set as 70 to indicate the priority of course change in collision avoidance maneuvering decision-making.

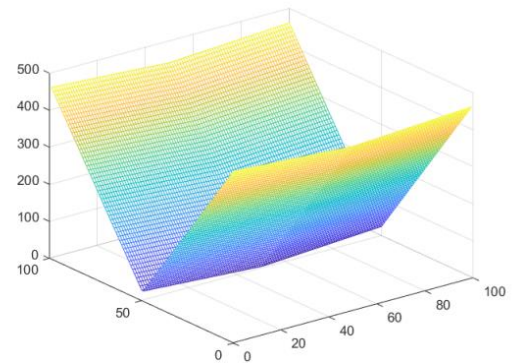
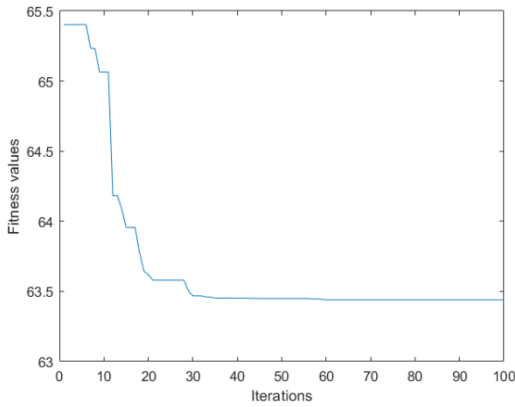


Figure 7 Collision avoidance function image

According to the requirements for collision avoidance actions in the COLREGs, this algorithm should make the collision avoidance actions large enough to be easily observed by other ship's visual and radar observation. Therefore, steering amplitude positioning (30°, 90°). The ship data is input into the collision avoidance algorithm based on improved PSO. The particle optimization image is shown in Fig. 7, and the optimization iteration process is shown in Fig. 8.





**Figure 8 Iterative process of collision avoidance algorithm**

The optimal fitness of the algorithm obtained through 30 iterations is 63.5, and the collision avoidance strategy obtained is that the ship turns 52° to the right. The speed change can be ignored because it is too small, so the it will not be changed. The ship sailed along this route for 14 minutes, and the ship S recovered its course after passing the starboard side of TS2, thus completing the collision avoidance maneuvering of the ship. TS2 encounters TS1 and TS3 in a cross situation, and encounters S in head-on, and TS2 is a yielding ship on the port side of TS1 and TS3. TS2 needs to implements steering right action for ships S, TS1 and TS3, pass the port side of S, and the stern of TS1 and TS2, to complete the collision avoidance operation. TS1 encounters S and TS2 in a cross situation, and needs to give way to S, that is, turn right and pass through the stern of S to avoid collision. TS3 and TS2 cross each other, but they are direct ships on the starboard side of TS2, basically maintaining the original course. Ship collision avoidance track is displayed in Fig. 9.

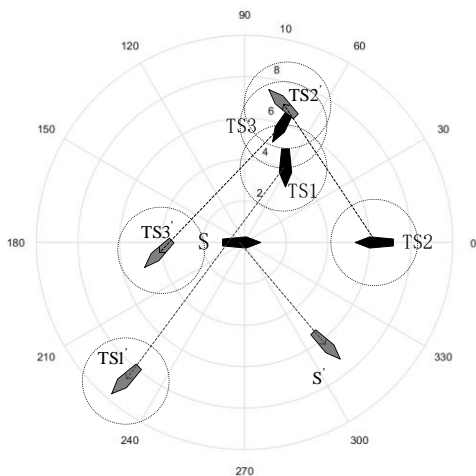


**Figure 9 Trajectory of ship collision avoidance**

**4.3 Simulation of ship collision avoidance path in narrow water**

For verification, the simulation platform of ship collision avoidance algorithm developed on Visual C++platform is used for experimental analysis. The number of particle swarm set in the simulation experiment is 50, and the number of iterations is 100. In the fitness function, m1 is set to 1 and m2 is set to 70.

According to the classification of collision avoidance in COLREGs, four meeting situations are simulated, as shown in Fig. 10, Fig. 11, Fig. 12, and Fig. 13.

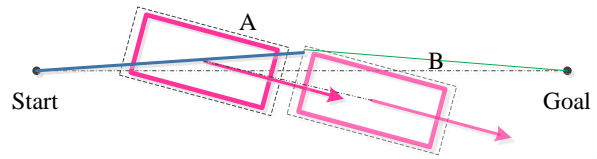


**Figure 10 Collision avoidance of overtaking**

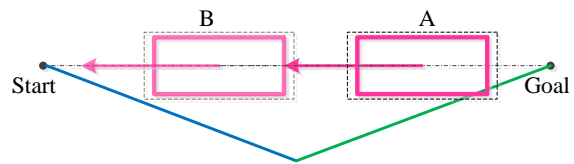


**Figure 11 Collision avoidance of head-on situation**

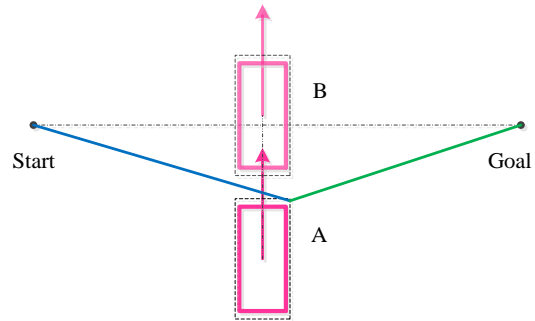


**Figure 12 Collision avoidance in starboard cross encounter situation**

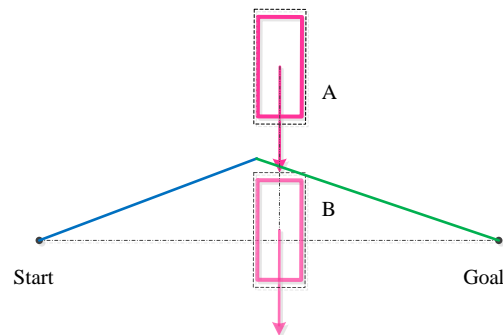


**Figure 13 Collision avoidance in stroke-side cross encounter situation**

"Start" refers to the position where the ship detects target ships and starts to avoid collision. "Goal" is the

recovery heading point after the ship completes collision avoidance. The state A is at the position of target ships when the own ship detects at the starting point "Start". State B of target ships refers to the position when the ship completes collision avoidance.

There are multiple static obstacles in the simulation environment, and there are circular obstacles of different sizes in the environment, which only reflects the static circular obstacle avoidance path planning, as shown in Fig. 14.

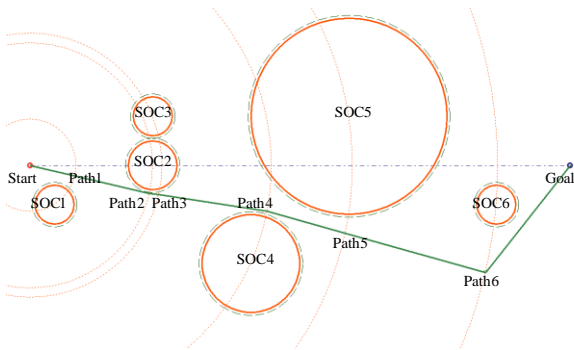


Figure 14 Ship planning path for circular obstacles

In this experimental simulation, it is assumed that the optimal path direction of the ship is due east. "Start" is the starting point, "Goal" is the ending point, the distance between the two points is 1100m, and the initial speed of the ship is 40kn. This value is used in the following simulation experiments. Six global optimal path nodes for static collision avoidance are obtained in Table 4. The environment contains six static circular obstacles, and their data shown in Table 5.

Table 4 Path node

Waypoint	Polar diameter/m	Polar angle /rad
1	94.34	6.041
2	250.00	6.041
3	269.26	6.060
4	492.44	6.083
5	657.65	6.051
6	953.36	6.021

Table 5 Circular obstacle parameters

Serial number	Polar diameter/m	Polar angle /rad	Diameter/m
SOC1	94.34	5.271	80
SOC2	250.00	0	100
SOC3	269.26	0.381	80
SOC4	492.45	5.865	200
SOC5	657.65	0.153	400
SOC6	953.36	6.199	80

There are multiple static obstacles in the simulation environment. There are five circular obstacles with different sizes and three static obstacles in the environment, which only reflects the static circular and rectangular obstacle avoidance path planning using the proposed method, as shown in Fig. 15.

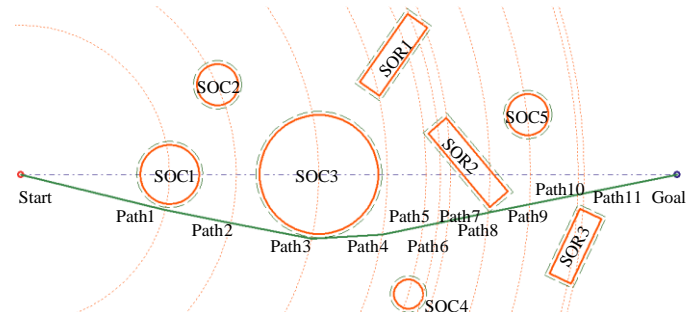


Figure 15 Ship planning path for multiple obstacles

Through path simulation on the platform, 11 global optimal path nodes for static collision avoidance and circular obstacle parameters are obtained in Table 6 and Table 7.

Table 6 Path node

Waypoint	Polar diameter/m	Polar angle /rad
1	250.00	6.042
2	362.5	6.058
3	500.0	6.067
4	615.10	6.120
5	680.07	6.156
6	704.14	6.167
7	721.96	6.175
8	787.85	6.202
9	855.86	6.225
10	935.62	6.247
11	945.13	6.250

Table 7 Circular obstacle parameters

Number	Polar diameter/m	Polar angle/rad	Diameter/m
SOC1	250.00	0.000	100
SOC2	362.49	0.427	70
SOC3	500.00	0.000	200
SOC4	680.07	5.850	50
SOC5	855.86	0.117	70

In order to simulate the situation of small obstacle density in narrow waters, a simulation collision avoidance environment is set up as shown in Fig. 16, which includes the two situations of encounter and cross encounter in the COLREGs, as well as the collision avoidance of some obstacle paths.

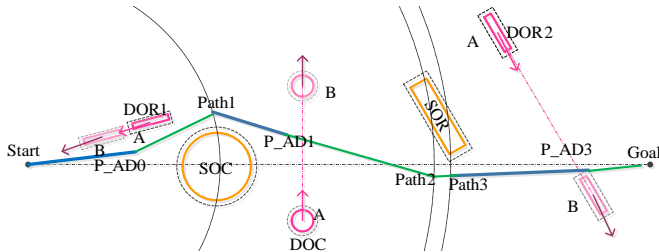


**Figure 16 Simulation analysis of ship collision avoidance path**

In this simulation experiment, three global optimal path nodes have been obtained in the parameters Table 8. The environment includes a static circular obstacle and a dynamic circular obstacle ship. Parameters of one static rectangular obstacle and two dynamic rectangular obstacle ships are shown in Table 9.

**Table 8 Path node**

Waypoint	Polar diameter/m	Polar angle/rad
1	350.00	0.226
2	649.28	0.010
3	669.83	0.002

At the starting time, to avoid the static circular obstacles and navigate along the first path point Path1, the dynamic rectangular obstacle ship DOR1 was detected, and the two ships were sailing in head-on. There was a risk of collision if they continued to navigate. Therefore, the ship needs to adjust its course, turn right and drive past the port side of the obstacle ship DOR1, with the speed unchanged. When reaching the end point of P\_AD0, the own ship will complete successful collision avoidance steering and continue to sail toward the first path point Path1.

**Table 9 Circular obstacle parameters**

Serial Number	Center Polar diameter r/m	Center Polar angle/rad	Diameter r/m	Speed/kn	Bearing angle (°)
SOC	350	0	100	-	-
DOC	468.4	6.002	30	20	90

When the ship reached the first path point Path1, it detected the dynamic circular obstacle ship DOC, and the two ships crossed each other. The ship is on its port side, so it needs to make way for it. According to the calculated collision avoidance strategy, the course is unchanged, the speed is reduced to 35.6kn, and the vehicle passes behind it. Reaching the end point of collision avoidance P\_AD1, the own ship completes the evasive action, and then gradually accelerates to

resume the speed and continues to sail toward the second path point, Path2. Rectangular obstacle parameters are displayed in Table10.

**Table 10 Rectangular obstacle parameters**

Serial Number	Center Polar diameter /m	Center Polar angle /rad	Half length /m	Half width /m	Bearing angle /(°)	Speed /kn
SOR	769.67	0.429	70	15	300	-
DOR1	445	0.833	28	4	200	17
DOR2	824	0.245	30	5	305	13

When the ship reaches the third path point Path3, it detects the dynamic rectangular obstacle ship DOR2, and other ships cross with the port side of the ship. According to the COLREGs, the ship is not a collision avoidance ship, so no action is required to maintain the course and speed. When it reaches the end point of collision avoidance P\_AD3, the collision risk is removed and the own ship continues to sail to the target point.

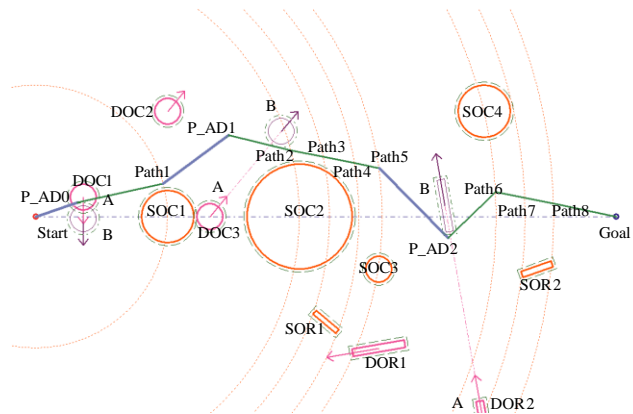


**Figure 17 Simulation analysis of ship collision avoidance path**

To simulate the situation of high obstacle density in narrow waters, a collision avoidance environment is set up as shown in Fig. 17. The simulation environment includes the overtaking and crossing situations, as well as the collision avoidance of some obstacle paths. In this simulation experiment, eight global optimal path nodes have been obtained in Table 12 with parameters.

The experimental environment includes four static circular obstacles and three dynamic circular target ships (some parameters are shown in Table 12). Two static rectangular obstacles and two dynamic rectangular obstacle ships (some parameters are shown

in Table 11).

**Table 11 Rectangular obstacle parameters**

Serial number	Centre Polar diameter/m	Centre Polar angle/rad	Half length /m	Half width /m	Bearing angle /( $^{\circ}$ )	Speed /kn
SOR 1	848.53	0.785	28	5	140	-
SOR 2	1118.03	0.464	30	6	200	-
DOR 1	955.25	0.748	50	7	190	40
DOR 2	1204.16	0.727	50	7	100	20

When the ship is sailing along the first path point Path1 under the global planning of the optimal path for static obstacles at the starting time, the dynamic circular obstacle ship DOC1 is detected later, and the two ships are sailing towards each other in a situation of cross encounter. The other ships are on the port side of the ship, so the ship is a straight sailing ship. However, in order to avoid the risk of collision, the ship needs to turn left, drive past the obstacle ship DOC1, and reach the collision avoidance end point P\_AD0 continues to navigate to the path point Path1.

**Table 12 Circular obstacle parameters**

Serial number	Polar diameter /m	Polar angle/rad	Diameter /m	Speed/kn	Bearing angle( $^{\circ}$ )
SOC1	250.00	0.000	100	-	-
SOC2	500.00	0.000	200	-	-
SOC3	657.65	6.131	50	-	-
SOC4	873.21	0.231	100	-	-
DOC 1	97.31	0.390	50	20	270
DOC 2	320.16	0.675	50	10	50
DOC 3	330.00	0.000	50	20	50

When the ship reaches the first path point Path1 during navigation, dynamic circular obstacle ships DOC2 and DOC3 are detected. There is no risk of collision between the ship and the dynamic circular obstacle DOC2. The ship and the dynamic circular obstacle DOC3 are in a overtaking situation, which means that the ship is overtaking DOC3 and the ship is on its port side. It is necessary to give way to the ship. Table 13 shows 8 path nodes.

**Table 13 Path node**

Waypoint	Polar diameter/m	Polar angle/rad
1	250.00	0.254
2	500.00	0.254
3	557.49	0.204
4	613.81	0.165
5	657.65	0.140
6	873.21	0.053
7	928.54	0.038
8	982.70	0.024

According to the calculated collision avoidance strategy, the ship turns  $23^{\circ}$  to the left, reduces its speed to 33 kn, drives past its rear, and reaches the collision avoidance end point P\_AD1 finished evading the dynamic obstacle ship DOC3, and then gradually accelerated to recover 40 kn and continued to sail to the second path point Path2.

When the ship reaches the fifth path point Path5, it detects the dynamic rectangular obstacle ship DOR2. Other ships cross the starboard side of the ship, and the ship is giving way. The calculated collision avoidance strategy is to turn right  $34^{\circ}$ , keep the speed unchanged, and after reach the end point of collision avoidance P\_AD5, continue to navigate to the path point Path6. Then it will drive to the end point of the global path "Goal" to complete global collision avoidance.

This improved PSO method plays a good role in solving multi-objective optimization problems, such as simple algorithm flow, simple parameters, and good convergence effect, when it is applied to ship collision avoidance in multiple ships or other complex situations. The optimal solution can be obtained only when the number of iterations does not exceed 30.

## 5. Conclusion

This paper aims at the requirements of collision avoidance and navigation safety for decision-making of ships during navigation. The ship encounter situation and the ship's collision avoidance responsibility are transformed into the constraints of collision avoidance decision-making. The simulation shows that the algorithm is not only applicable to single ship collision avoidance decision-making, but also can obtain reasonable strategies for multi ships collision avoidance decision-making.

An improved method was proposed to change the

inertia weight of PSO into an inertia weight that can change with the number of iterations. This method realizes the introduction of an adjustment factor into the inertia weight value, which effectively enhances the global search ability of the PSO algorithm in the early stage of the experimental iteration, and to a certain extent, enhances the local search ability in the late stage of the experimental iteration. Therefore, the improved PSO algorithm can have a strong ability to jump out of the local optimal solution after the cycle ends.

The collision avoidance model adopted geometric methods to convert the problem of ship collision avoidance path into the problem of ship speed change and course change. The fitness function is established based on the variable of ship speed change and direction. The target ship is modeled with the minimum safe encounter distance as the radius expansion considering bad weather conditions by using BP neural network.

The simulation results through MATLAB and Visual C++ show that the algorithm has strong reliability and fast solving speed. It is concluded that the ship collision avoidance system based on improved PSO has good effect of collision avoidance using an energy-saving path planning.

In the future research, the minimum safe meeting distance of ships can also be dynamically calculated for the classification of ship types. Besides, the navigation environment under the influence of weather will be considered.

### Acknowledgments

The authors sincerely thank the Editor-in-Chief, the Associate Editor, and the anonymous referees for their helpful and valuable comments. This work is partially supported by the Natural Science Foundation of China (No. 52101375), the Shandong Provincial Natural Science Foundation (ZR2021QG022, ZR2022ME087) the Hebei Province Natural Science Fund (No.E2021203142) and Shandong Jiaotong University PhD Startup foundation of Scientific Research, Shandong Province education science planning

innovative literacy special project (2022CYB260).

### References

- Durillo, J.J., Garcla-Nieto, J., Nebro, A.J., (2009), Multi-objective particle swarm optimizer: an experimental comparison, The 5th int. Conf. Evolutionary Optimization, Nantes, France, vol. 4, pp. 7-10.
- Fernandez-Martinez, J.L., Garcia-Gonzalo, E., (2011), Stochastic stability analysis of the linear continuous and discrete PSO models, IEEE Trans. Evol. Comput. vol. 15, no. 3, pp. 405-423.
- Ding J, Jin L, Chowdhury K R, Zhang W, Hu Q, Lei J. (2014), A particle swarm optimization using local stochastic search and enhancing diversity for continuous optimization, Neurocomputing, vol. 137, no. 5, pp. 261 – 267.
- Yong Z, Gong D W, Zhang J H. (2013), Robot path planning in uncertain environment using multi-objective particle swarm optimization, Neuro-computing, vol. 103, no. 1, pp. 172 – 185.
- Das, P.K., Behera, H.S., Panigrahi, B.K., (2016), A hybridization of an improved particle swarm optimization and gravitational search algorithm for multi-robot path planning-ScienceDirect, Swarm and Evolutionary Computation, vol. 28, pp. 14 – 28.
- Mac, T.T., Copot, C., Tran, D.T., (2017), A hierarchical global path planning approach for mobile robots based on multi-objective particle swarm optimization, Appl. Soft Comput. vol. 59, no. 1, pp. 68 – 76.
- Mistry, K., Zhang, L., Neoh, S.C., et al., (2017), A micro-GA embedded PSO feature selection approach to intelligent facial emotion recognition, IEEE T Cybern, vol. 47, no. 6, pp. 1496 – 1509.
- Agnieszka Lazarowska. (2014), Ship's trajectory planning for collision avoidance at sea based on ant colony optimisation, Journal of Navigation, vol. 68, no. 2, pp. 291 – 307.
- Jinfen Zhang, Di Zhang, Xinpeng Yan, Stein Haugen, C. Guedes Soares, (2015), A distributed anti-collision decision support formulation in multi-ship encounter situations under COLREGs, Ocean Engineering, vol. 105, pp. 336 – 348.
- Liang Hu, Wasif Naeem, Eshan Rajabally, Graham Watson, Terry Mills, Zakirul Bhuiyan, Ivor Salter, (2017), COLREGs-Compliant Path Planning for Autonomous Surface Vehicles: A Multiobjective Optimization Approach, IFAC-PapersOnLine, vol. 50, pp. 13662 – 13667.
- Chen L, Hopman H, Negenborn R R. (2018), Distributed model predictive control for vessel train formations of cooperative multi-vessel systems, Transportation Research Part

C: Emerging Technologies, vol. 92, pp. 101 – 118.

Chen, Linying, Negenborn, Rudy R., Hopman, Hans., (2018), Intersection crossing of cooperative multi-vessel systems, IFAC-PapersOnLine, vol. 51 , no. 9, pp. 379 – 385.

Chen L, Huang Y, Zheng H, Hopman HJJ, Negenborn RR. (2020), Cooperative Multi-Vessel Systems in Urban Waterway Networks, IEEE Transactions on Intelligent Transportation Systems, vol. 21, no. 8, pp. 3294 – 3307.

Wu, X., Bai, W., Xie, Y., (2018), A hybrid algorithm of particle swarm optimization, metropolis criterion and RTS smoother for path planning of UAVs, Appl. Soft Comput. vol. 73 , no. 10, pp. 735 – 747.

Su, S.J., Han, J., Xiong, Y.P., (2019), Optimization of unmanned ship' s parametric subdivision based on improved multi-objective PSO, Ocean. Eng. vol. 194 , no. 15, pp. 106617.

Shikai Shao, Yu Peng, Chenglong He, Yun Du, (2020), Efficient path planning for UAV formation via comprehensively improved particle swarm optimization, ISA Transactions, vol. 97, pp. 415 – 430.

Perera L P, Carvalho J P, Soares C G. (2014), Solutions to the failures and limitations of mamdani fuzzy inference in ship navigation, IEEE Transactions on Vehicular Technology, vol. 63, no. 4, pp. 1539 – 1554.

Hu Y, Meng X, Zhang Q, et al. (2020), A Real-time Collision Avoidance System for Autonomous Surface Vessel Using Fuzzy Logic, IEEE Access, vol. 99:1 – 1.

Yancai Hu, Gyei-Kark Park, (2020), Collision risk assessment based on the vulnerability of marine accidents using fuzzy logic, International Journal of Naval Architecture and Ocean Engineering, vol. 12, pp. 541-551.

Zhang W, Yan C, H Lyu, et al. (2021), COLREGS-based Path Planning for Ships at sea Using Velocity Obstacles, IEEE Access, vol. 99, pp. 1-14.

Guo X, Ji M, Zhao Z, et al. (2020), Global path planning and multi-objective path control for unmanned surface vehicle based on modified particle swarm optimization (PSO) algorithm, Ocean Engineering, vol. 216, no. 1, pp. 107693.

Abhishek B., Ranjit S., Shankar T., et.al. (2020), Hybrid PSO-HSA and PSO-GA algorithm for 3D path planning in autonomous UAVs, SN Applied Sciences, vol. 2, no. 11, pp. 1805.

Park J, Jeong J S. (2021), An Estimation of Ship Collision Risk Based on Relevance Vector Machine, Journal of Marine Science and Engineering, vol. 9, no. 5, pp. 538.

Akda M, Solnr P, Johansen T A. (2022), Collaborative collision avoidance for Maritime Autonomous Surface Ships:

A review, Ocean Engineering, vol. 250, pp. 110920.

Xiang Zuquan, Jin Chao, Du Kaijun, Mao Yunsheng, Song Lifei. (2015), Local Obstacle Avoidance for Unmanned Surface Vehicle Using a Hierarchical Strategy Based on Particle Swarm Optimization[J]. Journal of Wuhan University of Technology, 37 (07): 38 – 45.

Du Kaijun, Mao Yunsheng, Xiang Zuquan, Zhou Yongqing, Song Lifei, Liu Bin. (2015), A Dynamic Obstacle Avoidance Method of USV Based on COLREGS[J]. Shipbuilding Engineering, vol. 44, no. 03, pp. 119 – 124.

---

**Received 01 June 2023**

**Accepted 22 June 2023**